Spin redistribution by entanglement in an organic magnet

A. Zheludev, V. O. Garlea, S. Nishihara, Y.

Hosokoshi,³ A. Cousson,⁴ A. Gukasov,⁴ and K. Inoue⁵

¹HFIR Center for Neutron Scattering, Oak Ridge National Laboratory, Oak Ridge, Tennessee 37831-6393, USA.

²Department of Physical Science, Osaka Prefecture University, ,Osaka 599-8531, Japan.

³Department of Physical Science, Osaka Prefecture University,

Osaka 599-8531, Japan; Institute for Nanofabrication Research,

Osaka Prefecture University, Osaka 599-8531, Japan.

 $^4Laboratoire\ Leon\ Brillouin,\ CEA\text{-}CNRS\ Saclay,\ France.$

⁵Department of Chemistry, Hiroshima University, Hiroshima 739-8526, Japan.

A fundamental feature of quantum mechanics is entanglement [1, 2], defined as a physical realization of linear superpositions of simple multi-particle states. Entangled particles are physically interdependent even though they may be spatially separated. Experiments stimulated by potential applications in quantum computing [3, 4] have demonstrated the phenomenon using photons [5], other elementary particles [6], atoms [7, 8] and quasiparticles [9]. Entanglement of spin degrees of freedom in molecular magnets holds great promise for spintronics devices [10, 11, 12]. The simplest example is the ground state on an antiferromagnetic (AF) spin dimer. While neither spin points in any particular direction, their relative orientation remains strictly antiparallel [2]. More complex entangled states are realized in applied magnetic fields. For each magnetic atom or group of atoms the spin is quantized, and the magnetization can have only discrete values. Due to entanglement though, the spin density can be arbitrarily re-distributed, resulting in seemingly paradoxical fractional local magnetization. Below we report a direct quantifiable experimental observation of this effect in a novel organic molecular magnet.

The material in question, 2-[2',6'-difluoro-4'-(N-tert-butyl-N-oxyamino)phenyl]-4,4,5,5 - tetramethyl-4,5-dihydro-1H-imidazol-1-oxyl 3-oxide, F₂PNNNO for short, is a prototypical spin-tetramer system [13, 14]. Its molecular building block (Fig. 1a) contains only s- and p- elements, but is nevertheless magnetic, thanks to two unpaired electrons that reside in π^* antibonding molecular orbitals of the nitronyl nitroxide (NN) and the tert-butyl nitroxide (tBuNO) groups, respectively. These S=1/2 spins are coupled via a ferromagnetic intramolecular exchange constant $J_F \approx 35$ meV, as deduced from bulk susceptibility and magnetization measurements [14]. When in crystalline form, F₂PNNNO molecules are arranged in pairs, so that their tBuNO groups are close enough for AF interactions of magnitude $J_{AF} \approx 5.8$ meV [14]. The result is a two-molecule unit containing four interacting spins (Fig. 1b). Its unique ground state is a non-magnetic singlet with total spin $S_{\text{total}} = 0$ and a magnetization density that is strictly zero in entire space.

A non-trivial spin (magnetization) density is only to be found in some of the tetramer's excited states. In the presence of an external magnetic field applied along the z axis, the one with the lowest energy has a total spin $S_{\text{total}} = 1$ and a spin projection $S_{z,\text{total}} = +1$. We shall denote this state as $|1, +1\rangle$. Its wave function is heavily entangled: by diagonalizing

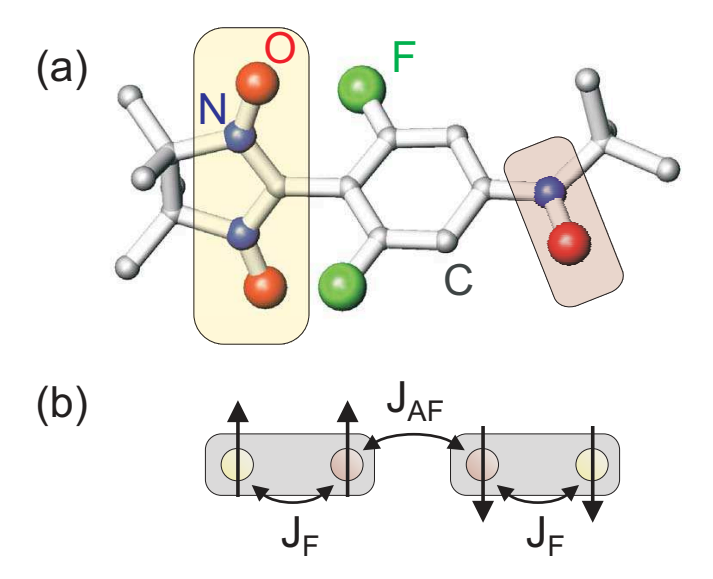


FIG. 1: (a) Molecular structure of F₂PNNNO. Hydrogen atoms are not shown. The shaded rectangles represent S=1/2-carrying unpaired electrons distributed over the nitronyl nitroxide and tert-butyl nitroxide groups. (b) A schematic representation of the 4-spin Heisenberg Hamiltonian for a two-molecule F₂PNNNO unit. J_F and J_{AF} are ferro- and antiferromagnetic exchange interactions, respectively. Vertical arrows represent individual spins in the classical ground state $|\uparrow\uparrow\downarrow\downarrow\rangle$. The actual quantum ground state has zero spin density throughout the tetramer.

the Heisenberg Hamiltonian of the tetramer we find that it actually is a linear combination of four "pure" (non-entangled) spin wave functions:

$$|1, +1\rangle = \alpha |\uparrow\uparrow\uparrow\downarrow\rangle + \beta |\uparrow\uparrow\downarrow\uparrow\rangle - \alpha |\downarrow\uparrow\uparrow\uparrow\rangle - \beta |\uparrow\downarrow\uparrow\uparrow\rangle, \tag{1}$$

where $\alpha \approx 0.46$ and $\beta \approx 0.54$. The most striking consequence of this entanglement is an imbalanced spin density distribution $S_z(\mathbf{r})$: the local spin populations of the NN groups are equal, but different from those of the tBuNO groups. The ratio R of these spin populations is given by $R = \alpha^2/\beta^2 \approx 1.39$. If entanglement was absent, and only pure spin-projection states were allowed, then, due to the weakness of the central antiferromagnetic bond, the lowest-energy excited state would have been $|\uparrow\uparrow\uparrow\uparrow\rangle$, with all spins equally saturated and $R_{\text{pure}} = 1$. If quantum mechanics failed altogether, the spins would behave as classical moments. They would align themselves in the (x,y) plane and tilt slightly in the field direction. It is easy to show that the resulting imbalance in $S_z(\mathbf{r})$ would be minuscule: $R_{\text{classical}} \approx 1 + |J_{\text{AF}}|/4|J_{\text{F}}| = 1.04$. Thus, a large imbalance of NN and tBuNO spin densities in F_2 PNNNO can be considered a signature of spin entanglement.

To observe this phenomenon, one must first prepare the tetramer in its first excited state. One strategy is to substantially increase the external field. Due to Zeeman effect, the energy of the excited state will decrease, and eventually reach zero at some critical field H_c . At this point it will become the new ground state, for which the spin density distribution can be measured. In F_2 PNNNO, due to residual inter-tetramer interactions, the transition at H_c is spread out between $H_1 = 9$ T and $H_2 = 15$ T [14]. While it is certainly possible to perform experiments at $H > H_1$, the equipment available for the present study was limited to fields up to 7 T. For this reason we used a slightly different approach. First, a high field was used to lower the energy of the $|1, +1\rangle$ state as much as possible. The data were then taken at an elevated temperature of T = 10 K that made this state partially populated due to thermal fluctuations. Of course, states $|1,0\rangle$ and $|1,-1\rangle$, as well as other higher-spin states got thermally excited as well. However, at T=10 K thermal populations of higher-spin states are negligible. The $|1,0\rangle$ state plays no role, as it has $S_z(\mathbf{r}) \equiv 0$. Finally, the spin density distribution in $|1,-1\rangle$ is exactly the reverse of that for $|1,+1\rangle$, and does not affect the imbalance between the NN and tBuNO groups. The main adverse effect of the finite-Tapproach is a reduction of the total magnetization of the tetramer, that ultimately reduces signal strength in any spin density measurement. For H = 7 T and T = 10 K we estimate the magnetization of the entire tetramer to be less than half of a Bohr magneton.

Measuring the distribution of such a small magnetization over two molecules with 48 atoms each with angstrom resolution is a formidable experimental challenge. It can only be met by polarized neutron diffraction [15]. This technique achieves great sensitivity by exploiting the interference between magnetic and nuclear scattering of neutrons in the crystal. In the experiment the so-called flipping ratios of 70 Bragg reflections were measured in F_2PNNNO in magnetic fields H=7 T and H=4 T. The magnitudes and signs (phases) of the corresponding spatial Fourier components of the spin density distribution were then extracted from these data. However, inverting the Fourier transform to reconstruct the real-space $S_z(\mathbf{r})$ function is far from straightforward, and prompted us to apply several complimentary approaches. One such tool was the maximum entropy (ME) method [16]. The procedure is model-independent: it uses only the experimental structure factors and crystal symmetry as input, and does not rely on any additional information or assumptions. It is known to be particularly effective at reconstructing 2D projections of $S_z(\mathbf{r})$ onto planes close to the principal scattering plane of the diffractometer [17]. Results of such reconstructions

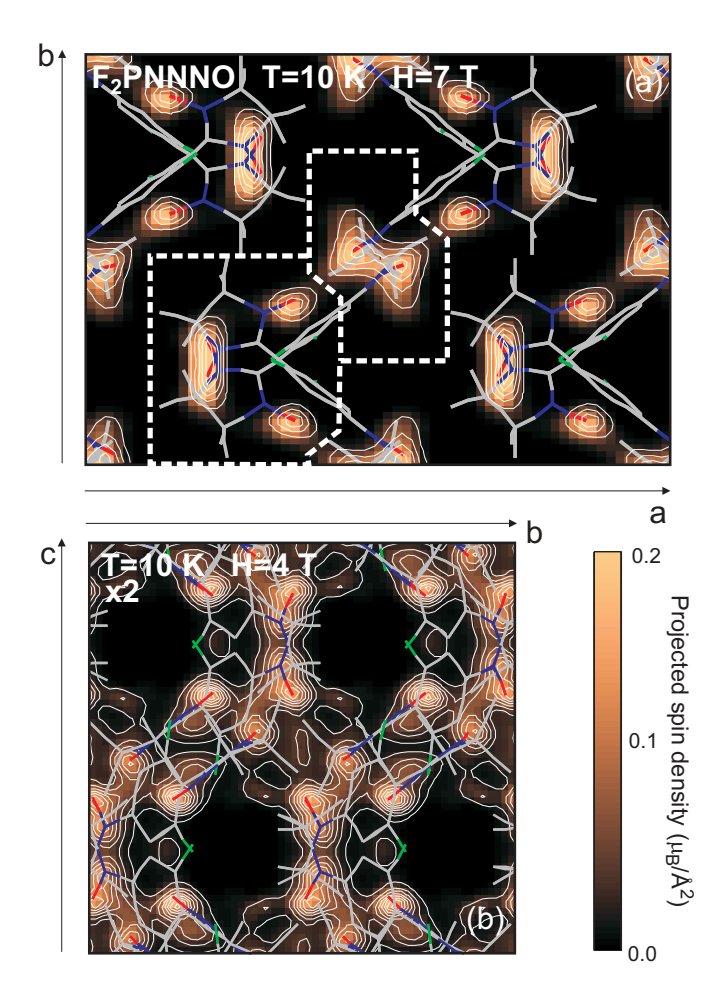


FIG. 2: Experimental spin density distribution in a F₂PNNNO spin-tetramer at T = 10 K, as reconstructed using the Maximum Entropy method. (a) and (b) are projections onto the (a, b) and (b, c) (crystallographic planes, respectively. Overlaid are skeletal representations of F₂PNNNO molecules as they are positioned within the crystallographic unit cell. Areas outlined with thick dashed lines were used to estimate the spin populations on the nitronyl nitroxide and *tert*-butyl nitroxide groups (see text).

for F_2PNNNO are shown in Fig. 2. Despite the limited experimental spatial resolution, one immediately sees that the spin density is primarily localized around the N and O atoms. Already at this stage it is possible to get a crude estimate of the redistribution effect. Integrating over the empirically chose regions outlined in Fig. 2a, we get R = 1.22, which clearly points to spin entanglement!

The actual NN/tBuNO spin population imbalance is likely to be even more pronounced than suggested by ME. For all its advantages, the algorithm is known to systematically

bias the answer towards a more uniform distribution. An alternative reconstruction method known as atomic orbital expansion (AOE) [15] lacks the benefit of being model-independent, but is free of such a bias and is better quantified. It involves refining a parameterized model for $S_z(\mathbf{r})$ to best-fit the experimental Fourier data. Its application to F_2 PNNNO was founded on previous experiments [18, 19, 20, 21] and first-principle calculations [18] for related nitroxides. The NN spin density was described in terms of five atomic populations. It was assumed to be concentrated in p_z Slater-type atomic orbitals of the O, N and apical C atoms, the z axis chosen perpendicular to the corresponding N-O-C planes. Two more parameters were used to quantify the spin density delocalized over the $p_{z'}$ orbitals of the tBuNO N and O atoms, with the z' axis perpendicular to the tBuNO O-N-C plane. One additional parameter was used for the sign-alternating spin density induced in the phenyl ring by virtue of the spin polarization effect [20, 21]. It was assumed to be contained in $p_{z''}$ orbitals of the phenyl's C atoms (z'' is oriented perpendicular to the phenyl plane). The final three parameters were the radial exponents of Slater-type atomic orbitals for the N, O and C atom types. This model yields an excellent least-squares fit to the data collected at $H=7~\mathrm{T}$ and $H=4~\mathrm{T}$, with $\chi^2=1.09$ and $\chi^2=1.20$, respectively. Figure 2 is an isosurface representation of the resulting 3-dimensional spin density distribution in the tetramer at $H=7 \mathrm{T}.$

A very good measure of the AOE's reliability is its result for the total tetramer magnetization: $m = 0.48(2)\mu_{\rm B}$ and $m = 0.28(2)\mu_{\rm B}$, for H = 7 T and H = 4 T, respectively, at T = 10 K. These values are consistent with existing bulk susceptibility data, and are in excellent agreement with a thermodynamic quantum-mechanical calculation for a single tetramer: $m = 0.59\mu_{\rm B}$ and $m = 0.32\mu_{\rm B}$, respectively. With this assurance of the validity of our approach, we can finally obtain experimental estimates for the imbalance between the NN and tBuNO spin populations: R = 1.53(3) and R = 1.51(2), for H = 7 T and H = 4 T, based on AOE model refinements. The observed magnitude of the effect is rather large. The quantitative agreement with theoretical predictions for entanglement-induced spin redistribution in F₂PNNNO is remarkable.

Our polarized neutron diffraction results not only provide a direct evidence of spin entanglement, but also help understand the microscopic interactions that cause it. In Fig. 3, note the negative density in the vicinity of the apical carbon atom of the NN group. This large negative spin population[20] plays a key role in the ferromagnetic intra-molecular coupling

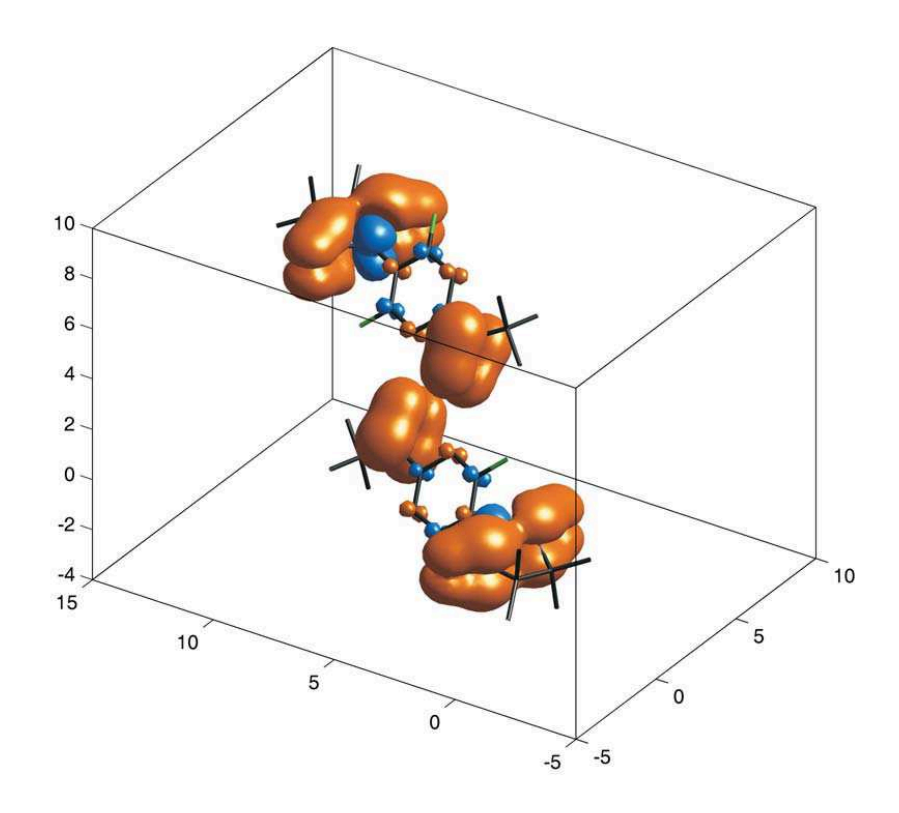


FIG. 3: Experimental spin density distribution in a F₂PNNNO spin-tetramer at H=7 T and T=10 K, as reconstructed using orbital model refinement (see text). The isosurfaces are drawn at $1\times 10^{-3}\mu_{\rm B}/{\rm Å}^3$ (orange) and $-1\times 10^{-3}\mu_{\rm B}/{\rm Å}^3$ (blue) levels. The axes show cartesian coordinates in Angstroms. The spin population of the central *tert*-butyl nitroxide groups are suppressed relative to those of the peripheral nitronyl nitroxides, due to entanglement caused by antiferromagnetic inter-molecular exchange interaction. Ferromagnetic intra-molecular interactions are mediated by a sign-alternating spin density wave that propagates across the phenyl rings and couples the nitronyl nitroxide- and *tert*-butyl nitroxide spins.

 $J_{\rm F}$. It is a part of a sign-alternating spin density wave that propagates across the phenyl ring and connects the positively populated N sites of the NN and tBuNO fragments over a large distance. This density-wave mechanism is analogous to Ruderman-Kittel-Kasuya-Yosida interactions in metals.[22, 23] Antiferromagnetic interactions $J_{\rm AF}$ between tBuNO groups of the two molecules comprising each tetramer span a shorter distance, and are more conventional in nature. They are due to direct exchange and arise from molecular orbital overlap.

The simplicity and isotropic nature of delocalized magnetic sp-electrons in organic molecules make them useful as a testing ground for fundamental quantum mechanics. In the particular case of F_2PNNNO we are able to detect and precisely quantify the redistribution of spin density caused by entanglement of four interacting quantum spins, and learn about the microscopic mechanisms of these entangling interactions.

Methods

Polarized neutron diffraction data were taken at the 5C1 and 6T2 lifting counter diffractometers installed at the Orpheé reactor at LLB, using 0.841 A and 1.4 A neutrons, respectively. Beam polarizations of 91 % or 97 % were achieved using Heussler-alloy monochromator and supermirror bender and and controlled by cryogenic flipper devices. A 20 mg F_2PNNNO single crystal sample was mounted consecutively with the a, b and c crystallographic axes parallel to the field direction. Crystal mosaic was better than 0.3* full width at half maximum. Sample environment was a 7 T cryomagnet. Overall, 70 independent flipping ratios were measured at T = 10 K, typically counting 2 hours per reflection on the 5C1 and 30 minutes on the 6T2 diffractometers, respectively.

In order to extract the magnetic structure factors from the measured flipping ratios, the low-temperature crystal structure of F_2PNNNO , including hydrogen atom positions, had to be determined. This was accomplished in a single crystal unpolarized neutron diffraction experiment. 3887 independent Bragg intensities were measured for a 5 mg single crystal sample on the 5C2 4-circle diffractometer at the Orphee using 0.832 Å neutrons. Sample environment was a gas flow cryostat, and the data were taken at T=50 K. The crystal structure was refined assuming isotropic vibrational parameters for hydrogen atoms, and general anisotropic ones for all other. The resulting least-squares R-factor was 0.089.

• The authors thank Dr. E. Ressouche (CEA Grenoble) for his expert assistance with the data analysis software. This work was supported (in part) under the auspices of the United States Department of Energy. The HFIR Center for Neutron Scattering is a national user facility funded by the United States Department of Energy, Office of Basic Energy Sciences- Materials Science, under Contract No. DE-AC05-00OR22725 with UT-Battelle, LLC. This work was supported in part by Grant-in-Aid for Scientific Research (B) No.18350076 and on priority Areas "High Field Spin Science in

- 100T" (No.451) from the Ministry of Education, Culture, Sports, Science and Technology (MEXT) of Japan.
- The authors declare that they have no competing financial interests.
- Correspondence and requests for materials should be addressed to A. Zheludev (email: zheludevai@ornl.gov).
- [1] Einstein, A., Podolsky, B. & Rosen, N. Can quantum-mechanical description of physical reality be considered complete? *Phys. Rev.* 47, 777–780 (1935).
- [2] Mermin, N. D. Is the moon there when nobody looks? reality and the quantum theory.

 Physics Today 38–47 (1985).
- [3] Lloyd, S. A. A potentially realizable quantum computer. Science 261, 1569–1571 (1993).
- [4] Bennett, C. H. & DiVincenzo, D. P. Quantum information and computation. *Nature* **404**, 247–255 (2000).
- [5] Freedman, S. J. & Clauser, J. F. Experimental test of local hidden-variable theories. Phys. Rev. Lett. 28, 938–941 (1972).
- [6] Lamehi-Rachti, M. & Mittig, W. Quantum mechanics and hidden variables: A test of Bell's inequality by measurement of the spin correlation in low-energy proton-proton scattering. *Phys. Rev. D* 14, 2543–2555 (1976).
- [7] Hagley, E. et al. Generation of Einstein-Podolsky-Rosen pairs of atoms. Phys. Rev. Lett. 79, 1–5 (1997).
- [8] Sackett, C. A. et al. Experimental entanglement of four particles. Nature 404, 256–259 (2000).
- [9] Chen, G. et al. Optically induced entanglement of excitons in a single quantum dot. Science **289**, 1906–1909 (2000).
- [10] Tejada, J., Chudnovsky, E. M., del Barco, E., Hernandez, J. M. & Spiller, T. P. Magnetic qbits as hardware for quantum computers. *Nanotechnology* 12, 181–186 (2001).
- [11] Leuenberger, M. N. & Loss, D. Quantum computing in molecular magnets. *Nature* **410**, 789–793 (2001).
- [12] Stamp, P. C. E. & Tupitsyn, I. S. Coherence window in the dynamics of quantum magnets. Phys. Rev. B 69, 014401 (2004).

- [13] Hosokoshi, Y. et al. Construction of S=1/2 Heisenberg ferromagnetic-antiferromagnetic alternating chains with various exchange couplings. J. Magn. Magn. Mater. 177-181, 634–635 (1998).
- [14] Hosokoshi, Y., Nakazawa, Y. & Inoue, K. Magnetic properties of low-dimensional quantum spin systems made of stable organic biradicals PNNNO, F2PNNNO, and PIMNO. *Phys. Rev.* B 60, 12924–12932 (1999).
- [15] Gillon, B. & Schweizer, J. Molecules in physics, Chemistry and Biology, 111 (Kluwer, 1989).
- [16] Papoular, R. J. & Gillon, B. Europhys. Lett 13, 429 (1990).
- [17] Papoular, R. J., Zheludev, A., Ressouche, E. & Schweizer, J. The inverse fourier problem in the case of poor resolution in one given direction: the maximum-entropy solution. *Acta Cryst.* A51, 295–300 (1995).
- [18] Zheludev, A. et al. Spin density in a nitronyl nitroxide free radical. Polarized neutron diffraction investigation and ab initio calculations. J. Am. Chem. Soc. 116, 2019–2027 (1994).
- [19] Zheludev, A. et al. Experimental spin density in the first purely organic ferromagnet: the beta para-nitrophenyl nitronyl nitroxide. J. Magn. Magn. Mater. 135, 147–160 (1994).
- [20] Davis, M. S., Morokuma, K. & Kreilick, R. W. Free radicals with large negative spin densities. J. Am. Chem. Soc. 94, 5588–5592 (1972).
- [21] Neely, J. W., Hatch, G. F. & Kreilick, R. W. Electron-carbon couplings of aryl nitronyl nitroxide radicals. J. Am. Chem. Soc. 96, 652–656 (1974).
- [22] Ruderman, M. A. & Kittel, C. Indirect exchange coupling of nuclear magnetic moments by conduction electrons. *Phys. Rev.* **96**, 99–102 (1954).
- [23] Yosida, K. Magnetic properties of Cu-Mn alloys. Phys. Rev. 106, 893–898 (1957).